JOURNAL OF Materials CHEMISTRY

Comparison of the structural behaviour of the low thermal expansion NZP phases $MTi_2(PO_4)_3$ (M = Li, Na, K)

D. A. Woodcock and P. Lightfoot*

School of Chemistry, University of St. Andrews, Purdie Building, North Haugh, St. Andrews, Fife, UK KY16 9ST. E-mail: pl@st-and.ac.uk

Received 25th May 1999, Accepted 18th August 1999

We present the results of high resolution neutron powder diffraction studies of the NZP phases $LiTi_2(PO_4)_3$ (LiTP) and $KTi_2(PO_4)_3$ (KTP). The thermal expansion coefficients for both materials are reported and compared to those of $NaTi_2(PO_4)_3$. α_a for LiTP is found to decrease from 0.75 to $0.27 \times 10^{-6}\,^{\circ}C^{-1}$ between 20 and 800 °C; α_c is found to be constant at $30.8 \times 10^{-6}\,^{\circ}C^{-1}$ over this temperature range. α_a for KTP is found to increase from -3.2 to $2.5 \times 10^{-6}\,^{\circ}C^{-1}$ over the same temperature range and α_V to increase from -0.8 to $12.8 \times 10^{-6}\,^{\circ}C^{-1}$. The anomalously large value of α_c in LiTP is related to the thermally induced migration of Li^+ from MI to MII sites, behaviour which is unique in these systems. Alamo's model for thermal expansivity in this system is applied and parameters reported.

Introduction

Many materials which exhibit the property of low or negative thermal expansivity are now known. These include microporous materials such as the pure SiO_2 zeolites ITQ-3,[1] chabazite,[2] and faujasite[3] and the aluminophosphates AlPO-5[4] and AlPO-17,[5] ZrW_2O_8[6] and materials with the $Sc_2(WO_4)_3$ structure type.[7–9] By far the most widely studied of such materials have been those with the NASICON structure.[10] Based on the material $NaZr_2(PO_4)_3$ (NZP), substitutions are possible leading to vastly differing thermal expansion properties ranging from contracting materials such as $NbTi(PO_4)_3$[11] (NbTP) to zero expansion $Ca_{0.25}Sr_{0.25}Zr_2(PO_4)_3$[12] (CaSrZP) and strong expansion $Ca_{0.25}Na_{0.5}Zr_2(PO_4)_3$.[13] NZP crystallises in the rhombohedral space group *R*-3*c*, consisting of corner sharing ZrO_6 octahedra and PO_4 tetrahedra forming $[Zr_2(PO_4)_3]$ units which align in chains up the *c* axis. Na^+ cations fill trigonal antiprismatic MI sites within these chains (Fig. 1).

The thermal expansivity within this system is generally anisotropic, with a contraction in *a* and expansion in *c* extremely common. Substitution of a divalent cation such as Ca or Sr for Na leads to an ordering of cations and vacancies in the MI sites, changing the symmetry to *R*-3 and also in most cases reversing the anisotropy and causing a contraction of *c* and expansion of *a vs.* temperature.

Oota and Yamai,[14] have studied a series of NZP materials such as LiZP, KZP and NZP, all of which showed a negative α_a and positive α_c, and showed a decrease in anisotropy when substituting larger ions for Na. Huang *et al.*[15] were the first to carry out a systematic study of MTP materials (Ti substituted for Zr in NZP), substituting Li, Na, K, Cs and Mg, Ca, Sr, Ba into the system. Huang's results also showed a correlation between ionic size and the thermal expansion properties.

Recent studies by Kutty *et al.*[16] varied the framework composition of the system and mentioned disorder from the MI site onto the extra framework MII sites, as shown in Fig. 1, as a possible explanation of the *c* axis contraction. However, our previous studies have shown no such disorder. Instead, we have investigated the length of the M–O bond and its effect on the MI site.[17] The behaviour of this site is critical to the thermal expansion properties of each material. Alamo[18] first proposed a model for the thermal expansivity of the system based on the expansion and contraction of this site. He had previously suggested the same model to explain the contraction of the *a* axis when substituting a larger cation into the room temperature structure. Lenain *et al.*[19] have developed the model to include Li, Na, K, Rb and CsZP and Rodrigo *et al.*[20] have studied a sample of NaTP using high temperature X-ray powder diffraction to confirm the model. It was also extended to include CaZP,[21] LiGeP[22] and NaSnP[23] in high temperature neutron powder diffraction studies. Detailed structural investigations have recently been carried out by us using variable temperature neutron powder diffraction on $NaTi_2(PO_4)_3$ (NaTP) and $Sr_{0.5}Ti_2(PO_4)_3$[17] (SrTP), $La_{0.33}Ti_2(PO_4)_3$[24] (LaTP), $NbTi(PO_4)_3$[11] (NbTP) and $Ba_{0.5}Ti_2(PO_4)_3$ (BaTP) and $K_{0.5}Nb_{0.5}Ti_{1.5}(PO_4)_3$[25] (KNTP). We have been able to apply the model to a more rigorous investigation which has enabled us to fully elucidate and understand the key factors influencing the thermal expansivity in these systems.

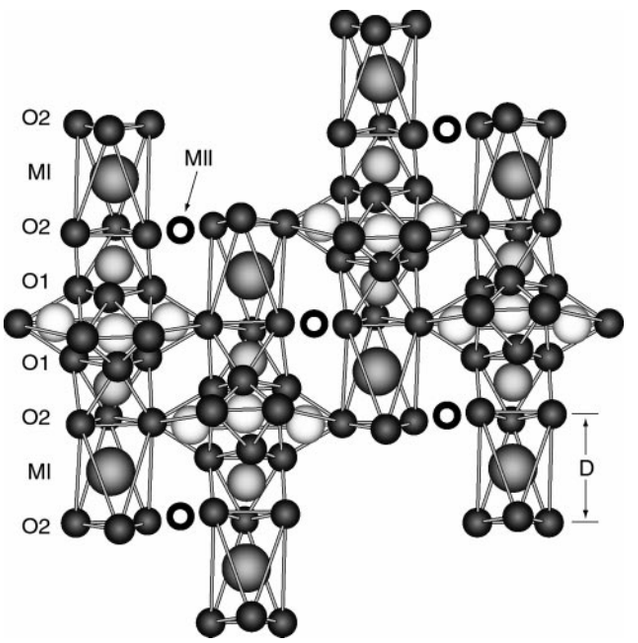

Fig. 1 Portion of the ideal NZP structure showing packing of polyhedral units along the *c* axis. MI and MII sites are shown. The parameter *D* refers to the distance between adjacent O2 planes along the *c* axis.

The present study compares $KTi_2(PO_4)_3$ (KTP) and $LiTi_2(PO_4)_3$ (LiTP), an important ionic conductor,[26] with the previously studied NaTP and provides the first detailed high temperature structural study of both materials. Both Alamo's model and the high temperature cation disorder in LiTP are investigated.

We also comment on the behaviour of the interpolyhedral Ti–O–P angles, which were identified by Evans *et al.*[7] as being an important factor in explaining the behaviour of some negative thermal expansion materials.

Experimental

Samples were synthesised using stoichiometric quantities of K_2CO_3 (Aldrich, 99+%), TiO_2 (Anatase, Aldrich, 99.9+%), Li_2CO_3 (Aldrich, 99+%) and $(NH_4)_2HPO_4$ (Aldrich, 99%). Starting materials were dried and ground under acetone before being heated in air to 200 °C for 18 h, 600 °C for 6 h and 900 °C for 12 h. Each sample was then pelleted and sintered for 24 h at 1000 °C followed by 24 h at 1100 °C and 24 h at 1150 °C. Sample purity was checked on a STOE STADI-P powder diffractometer operating in transmission mode using Cu-Kα_1 radiation.

Powder neutron diffraction data for both KTP and LiTP were obtained on the HRPD instrument at the ISIS facility, CLRC Rutherford Appleton Laboratory. Data were collected for 60 μA h at 20 °C then every 100 °C from 200 °C to 800 °C, again for 60 μA h at each temperature. Data were refined using the GSAS program[27] and typically consisted of 6308 data points, 38 variables, and 487 reflections over a *d*-spacing range of 0.705 to 2.49 Å for KTP and 6310 data points, 38 variables, and 474 reflections over a d-spacing range of 0.715 to 2.49 Å for LiTP. For all of these refinements a double-exponential pseudo-Voigt peak profile function was used. Anisotropic temperature factors were used for all refinements of KTP, although these led to unstable refinements in LiTP. This was due to the disordering of Li over two crystallographic sites as described later. In that case anisotropic temperature factors were used for Ti, P and O atoms only. Attempts to refine both isotropic temperature factors and site occupancies for Li led to unstable refinements, therefore both Li sites were constrained to have the same temperature factor as the isotropic equivalent on K in KTP at the same temperature. The occupancy of the MII site in LiTP was constrained to be equal to 1/3[1−occ.(MI)]. A typical Rietveld plot is shown in Fig. 2.

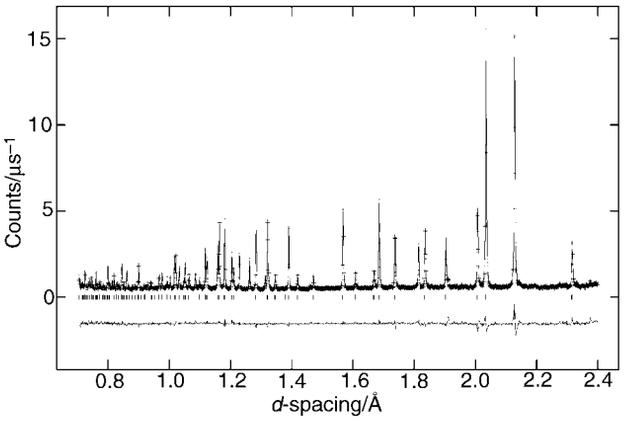

Fig. 2 A typical Rietveld plot for $LiTi_2(PO_4)_3$ at 20 °C.

Results and discussion

Coefficients of thermal expansion

The unit cell parameters and atomic co-ordinates at the highest and lowest temperatures are shown in Table 1 for LiTP and Table 2 for KTP. Plots of the thermal behaviour of unit cell parameters and volume are shown in Fig. 3. As can be seen, the behaviour of all parameters is non-linear. Polynomial coefficients of thermal expansion were therefore calculated using eqn. (1) and (2) below, where α is the coefficient of thermal expansion: $\alpha = 1/p\ \mathrm{d}P/\mathrm{d}T$.

$$p = p_2T^2 + p_1T + p_0 \quad (1)$$

$$\alpha = \frac{p_1 + 2p_2T}{p} \quad (2)$$

The resulting values for each material are tabulated in Table 3, and their coefficients of thermal expansion (CTEs) tabulated in Tables 4 and 5. These results are in very good agreement with those of Huang,[15] which are tabulated in Table 6. The overall conclusion is that substitution of a larger cation decreases the thermal expansion anisotropy (*i.e.* the difference between α_a and α_c). However, LiTP does shows near-zero *a* axis expansion, although its *c* axis expansion is significantly greater than that of NaTP (30.8 *cf.* $20.8 \times 10^{-6}\,^{\circ}\mathrm{C}^{-1}$). This unusual behaviour appears to be due to the disordering of Li from the MI to MII sites, as discussed below.

Disorder of Li

In LiTP there is a disordering of Li over the MI and MII sites which increases with temperature as shown in Table 1. LiTP remains the only material studied by us to show disordering of the MI cations onto the MII site. Moreover, a similar powder neutron diffraction study on $LiGe_2(PO_4)_3$ by Brochu *et al.*[22] did not show any evidence for occupancy of the MII site at any

Table 1 Experimentally determined atomic co-ordinates for $LiTi_2(PO_4)_3$[a]

Atom	Site	*x*	*y*	*z*	U_{eq}/Å^2
(a) at 20 °C. Space group *R*-3*c*, *a* = 8.51173(4) Å, *c* = 20.8524(2) Å. R_{wp} = 0.0715, R_p = 0.0701, χ^2 = 1.963					
Li	6b	0	0	0	3.47[b] occ. = 0.76(3)
Ti	12c	0	0	0.1412(2)	0.43(1)
P	18e	0.2907(3)	0	0.25	0.80(1)
O1	36f	0.1841(3)	−0.0044(3)	0.1901(1)	1.31(1)
O2	36f	0.1896(3)	0.1643(2)	0.0805(1)	0.97(1)
Li	18e	−0.323(9)	0	0.25	3.47[b] occ = 0.08(1)
(b) at 800 °C. Space group *R*-3*c*, *a* = 8.51541(3) Å, *c* = 21.3547(1) Å. R_{wp} = 0.0653, R_p = 0.0663, χ^2 = 2.111					
Li	6b	0	0	0	8.90[b] occ. = 0.37(3)
Ti	12c	0	0	0.1417(2)	1.69(1)
P	18e	0.2878(3)	0	0.25	2.15(1)
O1	36f	0.1778(3)	−0.0180(3)	0.1914(1)	4.31(1)
O2	36f	0.1923(2)	0.1647(2)	0.0857(1)	3.70(1)
Li	18e	−0.2800(4)	0	0.25	8.90[b] occ. = 0.21(1)

[a]Full listings of anisotropic thermal parameters and bond distances and angles are available from the authors. [b]Temperature factors on Li were constrained to be equal to those for equivalent temperatures for K in KTP to stabilise refinements.

Table 2 Experimentally determined atomic co-ordinates for $KTi_2(PO_4)_3$[a]

Atom	Site	x	y	z	U_{eq}/Å^2
(a) at 20 °C. Space group $R\bar{3}c$, $a=8.35694(3)$ Å, $c=23.0724(2)$ Å. $R_{wp}=0.0805$, $R_p=0.0800$, $\chi^2=3.275$.					
K	6b	0	0	0	3.47(1)
Ti	12c	0	0	0.1490(2)	0.86(1)
P	18e	0.2827(3)	0	0.25	1.20(1)
O1	36f	0.1539(2)	−0.0549(2)	0.1975(1)	1.71(1)
O2	36f	0.1982(2)	0.1676(2)	0.0986(1)	1.80(1)
(b) at 800 °C. Space group $R\bar{3}c$, $a=8.35431(2)$ Å, $c=23.19006(9)$ Å. $R_{wp}=0.0647$, $R_p=0.0619$, $\chi^2=2.278$.					
K	6b	0	0	0	8.90(2)
Ti	12c	0	0	0.1498(2)	2.13(1)
P	18e	0.2835(2)	0	0.25	2.65(1)
O1	36f	0.1545(3)	−0.0551(2)	0.1980(1)	4.49(1)
O2	36f	0.1989(2)	0.1684(2)	0.0991(1)	4.43(1)

[a]Full listings of anisotropic thermal parameters and bond distances and angles are available from the authors.

temperature. This disordering effect had been suggested by Kutty *et al.*[16] as being a possible explanation for the *c* axis contraction in SrZP. LiTP however, exhibits the strongest *c* axis expansion of any material studied by us (30.8×10^{-6} °C^{-1}), which does not appear to follow from this suggestion. Delmas *et al.*[28] carried out a full structural study of $Li_3Ti_2(PO_4)_3$ and found that all the Li cations occupied the MII sites in preference to the MI sites. On comparing $LiTi_2(PO_4)_3$ to $Li_3Ti_2(PO_4)_3$ they observed an increase in the *c* axis but a decrease in the *a* axis. They suggested that the increased repulsion between the layers of oxygen ions around MI led to a much larger *c* parameter. In this case it would appear that disordering of the Li cations onto the MII sites produces the same effect, leading to a larger than expected α_c. LiTP shows by far the greatest expansion in the MI site size (defined as *D*, the O2–O2 distance along the *c* axis[17]), expanding from 3.36(1) to

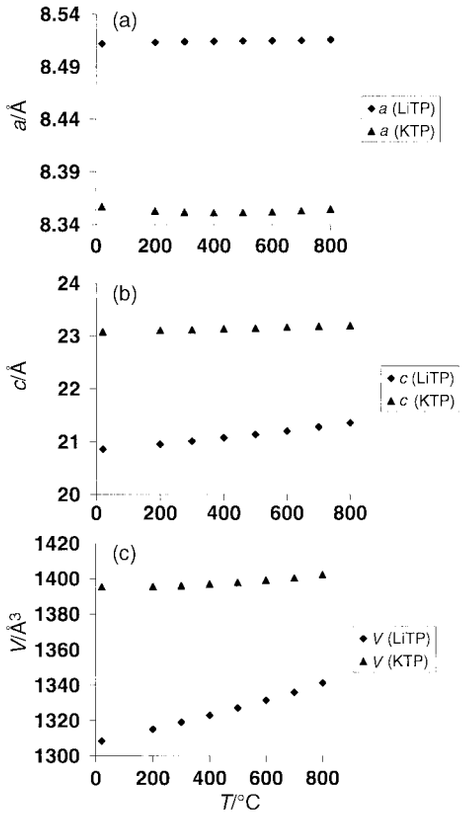

Fig. 3 Thermal evolution of lattice parameters for LiTP and KTP; (a) *a* axis, (b) *c* axis, (c) unit cell volume.

Table 3 Experimentally determined polynomial parameters

Axis	p_2	p_1	p
a_{KTP}	3.0255×10^{-8}	-2.7662×10^{-5}	8.3513
c_{KTP}	2.0119×10^{-8}	1.3501×10^{-4}	23.069
V_{KTP}	1.22016×10^{-5}	-1.6061×10^{-3}	1395.4
a_{LiTP}	-2.5956×10^{-9}	6.471×10^{-6}	8.5112
c_{LiTP}	0	6.4172×10^{-4}	20.824
V_{LiTP}	1.0003×10^{-5}	3.3204×10^{-2}	1307.9

Table 4 Experimentally determined CTEs for KTP ($\times10^{-6}$ °C^{-1})

T	α_a	α_c	α_V	α_L[a]
20	−3.20	5.89	−0.8	−0.27
200	−1.90	6.20	2.35	0.78
300	−1.10	6.38	4.10	1.37
400	−0.41	6.55	5.84	1.95
500	0.31	6.72	7.59	2.53
600	1.04	6.90	9.34	3.11
700	1.76	7.07	11.1	3.70
800	2.48	7.25	12.8	4.27

[a]$\alpha_L=1/3\alpha_V$.

3.66(1) Å compared to 3.90(1) to 4.08(1) Å in NaTP and 4.55(1) to 4.60(1) Å in KTP. The MI–O bond expands from 2.264(2) to 2.388(2) Å in LiTP compared to 2.466(4) to 2.569(5) Å in NaTP and 2.749(2) to 2.773(2) Å in KTP. It is normal in NZP systems for a positive α_c to lead to a negative α_a, *via* couple rotations of linked polyhedra. In this case it would appear that this tendency is counterbalanced by the increasing occupancy of the MII sites, which acts to inhibit *a* axis contraction, leading to the observed near zero α_a.

The Alamo model

As mentioned earlier, it is the expansion and contraction of the occupied and vacant MI sites which drives the co-operative rotations of linked tetrahedra and octahedra. The Alamo model breaks down the overall expansivity along both the *c* and the *a* axes into individual contributions from the TiO_6 and PO_4 polyhedra. Very little change in the bond lengths within these polyhedra is observed with temperature, and the expansivity is therefore described in terms of rotations and distortions of the polyhedra. The TiO_6 octahedron lies on a 3-fold axis along *c*, and its projection is shown in Fig. 4. ϕ_1 and ϕ_2 define rotations of the 'upper' and 'lower' O_3 planes around the

Table 5 Experimentally determined CTEs for LiTP ($\times10^{-6}$ °C^{-1})

T	α_a	α_c	α_V	α_L[a]
20	0.748	30.8	25.7	8.57
200	0.638	30.8	28.5	9.50
300	0.577	30.8	30.0	10.0
400	0.516	30.8	31.5	10.5
500	0.455	30.8	33.1	11.0
600	0.394	30.8	34.6	11.5
700	0.333	30.8	36.1	12.0
800	0.272	30.8	37.7	12.6

[a]$\alpha_L=1/3\ \alpha_V$.

Table 6 Comparison of average CTEs with Huang's results[15]

	$\alpha_a/\times10^{-6}$ °C^{-1}	$\alpha_c/\times10^{-6}$ °C^{-1}
LiTP (this work)	0.49	30.8
LiTP (ref. 15)[a]	−0.05	30.59
NaTP (this work)	−5.3	20.8
NaTP (ref. 15)[a]	−3.88	20.74
KTP (this work)	−0.13	6.62
KTP (ref. 15)[a]	0.21	5.73

[a]$T=25$–1000 °C.

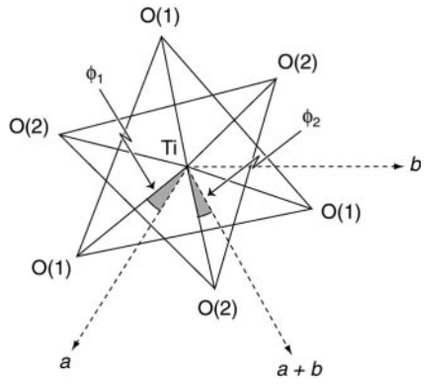

Fig. 4 Projection of a TiO_6 octahedron along the 3-fold axis (*c* axis).

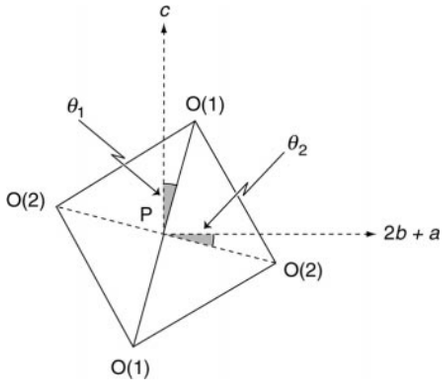

Fig. 5 Projection of a PO_4 tetrahedron along the 2-fold axis (*a* axis).

c axis. The PO_4 tetrahedron lies on a 2-fold axis in space group *R*-3*c*. Corresponding rotation angles in this polyhedron are shown in Fig. 5— θ_1 and θ_2. The angles Ω and Δ are a measure of the distortion of the octahedra and tetrahedra, calculated as follows:

$$\Omega = \phi_1 - \phi_2 + 60^\circ \quad (3)$$

$$\Delta = \theta_2 - \theta_1 + 90^\circ \quad (4)$$

The expansivities of the TiO_6 and PO_4 polyhedra are insignificant over the temperature range studied. Values of the parameters ϕ_1, ϕ_2, θ_1, θ_2, Δ, and Ω for LiTP and KTP as a function of temperature are shown in Fig. 6. In LiTP ϕ_1 increases strongly and ϕ_2 increases only slightly, leading to an increase in Ω, the octahedron becoming more regular. The values of these changes are almost identical to those in NaTP.[24] However in KTP, both ϕ_1 and ϕ_2 remain virtually constant, leading to no change in Ω.

Consideration of the angles relating to the tetrahedra (θ_1 and θ_2) shows the same trend: a great similarity between NaTP and LiTP and a difference from KTP. θ_1 and θ_2 both increase strongly at much the same rate in both NaTP and LiTP, leading to a virtually rigid PO_4 tetrahedron. Within KTP, θ_1 remains constant and θ_2 increases very slightly leading to a small increase in Δ. Overall it appears that there is little distortion of the tetrahedra, but that these rotate in LiTP and NaTP, but remain in the same position in KTP. It is likely that the relatively small changes in the Alamo parameters for KTP result from the fact that these values (*i.e.* ϕ and θ) are quite high in the room temperature structure. In other words, the structure is already under severe strain and distortion due to the large size of the MI site, and will not distort much further, hence the relatively smaller values of α_a and α_c for KTP *vs.* NaTP.

Consideration of Ti–O–P angles

Evans *et al.* have suggested that interpolyhedral angles (M–O–M′) change significantly in some negative thermal expansion materials.[7] The angle Ti–O1–P in both LiTP and KTP remains constant, as does Ti–O2–P in KTP (Fig. 7). However, Ti–O2–P in LiTP shows a large increase. Our previous studies on NbTP[11] showed a small contraction in *a* and expansion in *c*, but little change in either Ti–O–P angle; any change was smaller than the Rietveld esds. These angles do not change enough to be an indicator for the thermal expansion properties in the NZP family.

Conclusions

In LiTP, there is a significant disordering of Li cations from the MI to MII site on heating which had not been previously reported from X-ray diffraction studies and has not been seen in any other NZP phases. This phenomenon resembles that observed in changing from $LiTi_2(PO_4)_3$ to $Li_3Ti_2(PO_4)_3$, in which the former has the MI sites fully occupied and the latter the MII sites fully occupied. Consequently, α_c for LiTP is very high due to relaxation of the MI sites from a very small size ($D = 3.36$ Å) to a larger size ($D = 3.66$ Å) as Li migrates from

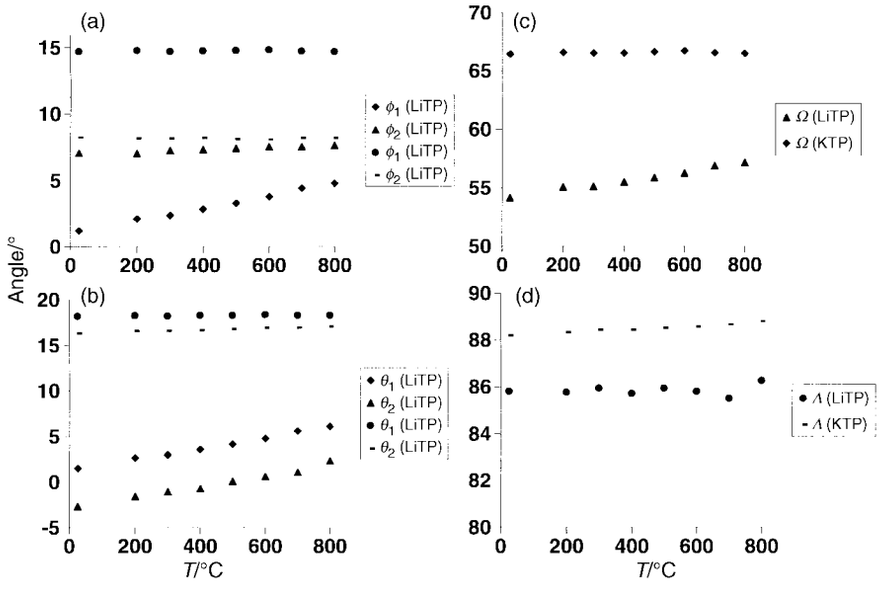

Fig. 6 Variation of the parameters from the Alamo model; (a) ϕ_1 and ϕ_2, (b) θ_1 and θ_2, (c) Ω, (d) Δ.

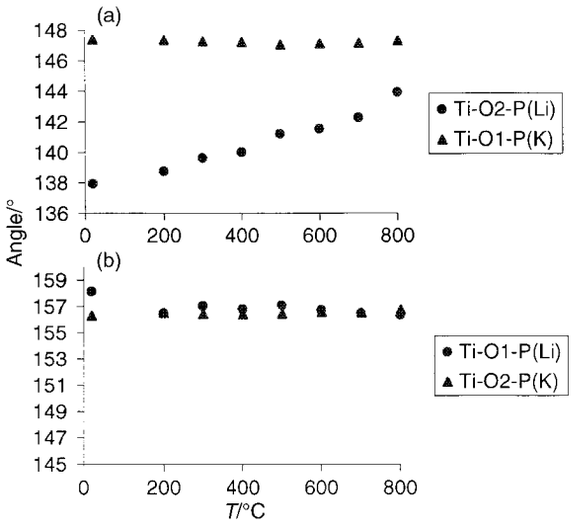

Fig. 7 Thermal evolution of the interpolyhedral Ti–O–P angles for KTP and LiTP.

MI to MII sites. Comparing the series LiTP, NaTP, KTP in terms of increasing cation size, the results are in agreement with those of Huang, in that as the cation size increases thermal expansivity decreases. This effect appears to be due to the amount of 'strain' present in the structure with respect to MI cation size; for the larger K^+ cation the MI site is large, polyhedral tilts (ϕ and θ) are consequently large, and changes in ϕ and θ are small, leading to the smaller α_a and α_c values.

Acknowledgements

We would like to acknowledge the EPSRC for provision of a studentship to D.A.W. and access to the ISIS facility and to thank Dr Richard Ibberson and Miss Zoe Lethbridge for assistance in collection of neutron diffraction data.

References

1 D. A. Woodcock, P. Lightfoot, P. A. Wright, L. A. Villaescusa, M.-J. Díaz-Cabañas and M. A. Camblor, *J. Mater. Chem.*, 1999, **9**, 349.
2 D. A. Woodcock, P. Lightfoot, L. A. Villaescusa, M.-J. Díaz-Cabañas, M. A. Camblor and D. Engberg, *Chem. Mater.*, in press.
3 M. P. Attfield and A. W. Sleight, *Chem. Commun.*, 1998, 601.
4 S. H. Park, R. W. Groβe Kunstleve, H. Graetsch and H. Gies, *Stud. Surf. Sci. Catal.*, 1997, **105**, 1989.
5 M. P. Attfield and A. W. Sleight, *Chem. Mater.*, 1998, **10**, 2013.
6 J. S. O. Evans, T. A. Mary, T. Vogt, M. A. Subramanian and A. W. Sleight, *Chem. Mater.*, 1996, **8**, 2809.
7 J. S. O. Evans, T. A. Mary and A. W. Sleight, *J. Solid State Chem.*, 1998, **137**, 148.
8 D. A. Woodcock, P. Lightfoot and C. Ritter, *J. Solid State Chem.*, in press.
9 J. S. O. Evans, T. A. Mary and A. W. Sleight, *J. Solid State Chem.*, 1997, **133**, 580.
10 J. P. Boilot, J. P. Salanie, G. Desplanches and D. Le Potier, *Mater. Res. Bull.*, 1979, **14**, 1469.
11 D. A. Woodcock, P. Lightfoot and R. I. Smith, *Mater. Res. Soc. Symp. Proc.*, 1998, **547**, 191.
12 S. Y. Limaye, D. K. Agrawal and H. A. McKinstry, *J. Am. Ceram. Soc.*, 1987, **70**, C232.
13 R. Roy, D. K. Agrawal, J. Alamo and R. A. Roy, *Mater. Res. Bull.*, 1984, **19**, 471.
14 T. Oota and I. Yamai, *J. Am. Ceram. Soc.*, 1986, **69**, 1.
15 C. Y. Huang, D. K. Agrawal and H. A. McKinstry, *J. Mater. Sci.*, 1995, **30**, 3509.
16 K. V. G. Kutty, R. Asuvathraman and R. Sridharan, *J. Mater. Sci.*, 1998, **33**, 4007.
17 D. A. Woodcock, P. Lightfoot and C. Ritter, *Chem. Commun.*, 1998, 107.
18 J. Alamo, *Solid State Ionics*, 1993, **63–65**, 547.
19 G. E. Lenain, H. A. McKinstry, J. Alamo and D. K. Agrawal, *J. Mater. Sci.*, 1987, **22**, 17.
20 J. L. Rodrigo, P. Carrasco and J. Alamo, *Mater. Res. Bull.*, 1989, **24**, 611.
21 J. Alamo and J. L. Rodrigo, *Solid State Ionics*, 1993, **63–65**, 678.
22 M. Alami, R. Brochu, J. L. Soubeyroux, P. Gravereau, G. Le Flem and P. Hagenmuller, *J. Solid State Chem.*, 1991, **90**, 185.
23 J. Alamo and J. L. Rodrigo, *Mater. Res. Bull.*, 1992, **27**, 1091.
24 P. Lightfoot, D. A. Woodcock, J. D. Jorgensen and S. Short, *Int. J. Inorg. Mater.*, 1999, **1**, 53.
25 D. A. Woodcock, P. Lightfoot and R. I. Smith, *J. Mater. Chem.*, 1999, **9**, 2631.
26 H. Aono, E. Sugimoto, Y. Sadaoka, N. Imanaka and G. Adachi, *J. Electrochem. Soc.*, 1990, **137**, 1023.
27 A. C. Larson and R. B. Von Dreele, Report No. LA-UR-86-748, Los Alamos National Laboratory, Los Alamos, NM, 1987.
28 C. Delmas, A. Nadiri and J. L. Soubeyroux, *Solid State Ionics*, 1988, **28–30**, 419.

Paper 9/04193A